



Comparative Analysis of Microstrip Antenna Arrays with Diverse Feeding Techniques

**Obiadi Ifeanyi F. ^a, Udofia Kufre M. ^{a*}
and Udofia Kingsley M. ^a**

^a *Department of Electrical and Electronics Engineering, University of Uyo, Uyo, Nigeria.*

Authors' contributions

This work was carried out in collaboration among all authors. All authors read and approved the final manuscript.

Article Information

DOI: 10.9734/JERR/2024/v26i11060

Open Peer Review History:

This journal follows the Advanced Open Peer Review policy. Identity of the Reviewers, Editor(s) and additional Reviewers, peer review comments, different versions of the manuscript, comments of the editors, etc are available here: <https://www.sdiarticle5.com/review-history/111205>

Original Research Article

Received: 29/10/2023

Accepted: 05/01/2024

Published: 09/01/2024

ABSTRACT

A robust antenna design and analysis to fit the growing technology trend and give engineers and technicians options is crucial. This is especially true considering the recent rise in wireless smart devices. This paper compares microstrip antenna arrays fed in different ways. This work designed, simulated, and analyzed six antennas: two single-band rectangular microstrip antennas (RMSAs) with quarter wave (QWT) feed and the other with inset feed, one series-fed 1 x 4 RMSA array, two cooperate-fed (1 x 2 and 1 x 4) and a 2 x 2 cooperate-series-fed RMSA array at 2.4 GHz. Simulations showed that single-band antennas achieved 65.3 MHz and 68.3 MHz (2.72% and 2.85%) fractional bandwidths at 2.4 GHz. Series-fed and cooperative-fed 1 x 4 arrays, respectively, achieved bandwidths of 152.07 MHz and 44.33 MHz (6.34 % and 1.85 %) fractional bandwidth. The 1 x 2 cooperate-fed and 2 x 2 cooperate-series-fed array antennas had bandwidths of 33.06 MHz and 50.41 MHz (for 1.38% and 2.26%), respectively. A comparison of antenna gains revealed that the study's goals were met as a result of the realized antenna gain of the 2 x 2 cooperate-series-fed antenna which exceeded all other compared antenna gain. The 1 x 4 RMSA array with series

*Corresponding author: Email: kufremudofia@uniuyo.edu.ng;

feeding had a significantly higher bandwidth than its studied contemporaries. The achieved antenna's bandwidth qualifies it for application small ISM-band WLAN devices; for less portable devices, 2×2 hybrid-fed array antenna is a suitable candidate for application.

Keywords: Microstrip; array antenna; cooperative-fed; series-fed; bandwidth; inset-fed.

1. INTRODUCTION

Antennas play a fundamental role in wireless communication systems. The majority of antenna applications—and the sector in which they are most commonly found—are in telecommunications [1]. According to [2], whereas a transmission line requires a guiding structure (typically one conductor), antennas require no guiding structure. As defined by [3], an antenna is an electrical device that uses electric power input to create radio waves, which are then intercepted by the receiver side and converted back into electrical energy. This allows the antenna to transmit electromagnetic waves into space. For an antenna to be suitable for application in contemporary wireless devices, some characteristics such as low profile, easy fabrication, moderate gain and high radiation efficiency have to be met [4–7].

Microstrip antennas, also referred to as printed antennas, are antennas used in telecommunications; they are etched on printed circuit boards (PCBs) using a photolithographic method [8,9]. According to [10], microstrip antenna offers desirable flexibility and versatility in terms of fields of application. Their natural qualities—such as their robustness, low-profile structure, low cost of production, and lightweight nature—are mostly responsible for this. Microstrip antennas (MSAs) are incredibly versatile, although their gain and bandwidth performance are constrained [11].

A wide variety of feeding strategies are available for providing power to antennas; of these strategies, only two broad categories are applicable to microstrip antennas, viz: contacting and non-contacting method [12]. In a contacting approach, the RF power is provided directly to the radiating patch through a connecting device such as a microstrip line. In the non-contacting scheme, power is transferred via electromagnetic field coupling between the microstrip line and the radiating patch.

Different authors have proposed quite a number of methods to improve the performance of MSAs. As stated by [13], array configuration is usually

adopted to enhance the gain of MSAs. However, [14] in his work reported that the array feed, to a large extent, determines the gain improvement achieved. In this paper, MSA arrays with diverse feeding techniques are presented with the aim of understanding the effect of the feeding scheme on the realized gain.

The remainder of this paper is organized as follows. Section 2 presents a review of related literature. The MSA design methodology is explained in detail in Section 3. Result analysis of the designed MSA is presented in Section 4. Finally, the paper is concluded in Section 5 with list of references used in the study appended thereafter.

2. REVIEW OF RELATED LITERATURE

Numerous research papers have reported on a series of rectangular microstrip antenna arrays. These researchers, in order for them to obtain their antenna's performance parameters, adopted diverse design techniques, configurations, and electromagnetic simulators.

Ali and Khawaja [15] presented the design, optimization and simulation of a dual-band coaxial-fed 2×2 rectangular U-slot microstrip patch antenna array for wireless sensor network applications with operating frequencies of 2.1 GHz and 3.5 GHz. Their antenna was designed to be compliant with multiple-input-multiple-output (MIMO) applications for high-speed wireless sensor networks (WSNs) based communication standards that operates within 1-5 GHz frequency range. Antenna simulation was performed in Agilent Advanced Design System (ADS) Momentum using Rogers TMM3 substrate ($\epsilon_r = 3.27$ and substrate thickness, h of 6.35 mm). Minimum return losses of -19 dB and -17 dB was achieved at 2.1 GHz and 3.5 GHz. The highest gain of 11 dBi was achieved by the 2×2 U-slot rectangular patch antenna array proposed at 2.1 GHz. Though the antenna met its design objectives, no explicit design equation was shown for the patch, U-slot on the patch, and the patch feed and as stated by the authors, all optimization of the antenna was done on the software platform hence the absence of actual

design calculations negating established standard for use of antenna design equations.

Sohail [16] proposed a 4 x 4 microstrip patch antenna array for near field focused operation at 2.4 GHz at 800 mm from the reference origin. The 36 mm x 28 mm rectangular patch antenna was inset fed on FR-4 dielectric. The substrate was 1.6 mm thick. The antenna array resonated at 2.39 GHz with -56 dB return loss. At 2.4 GHz, return loss was -17 dB, below the threshold of -10 dB. The report stated that the author's antenna had a 50 MHz -10 dB bandwidth. Shifting each element's phase relative to the reference point focused antenna radiation at the focal point. Maximum radiation from aperture was 350 mm for a focused MPA array.

A 1 x 4 linear inset fed rectangular microstrip antenna array to increase directivity, gain and efficiency at 2.4 GHz was presented by [17]. The antenna achieved antenna gain of 13.2 dB signifying a good performance as compared to single patch antenna with nominal gain of between 5 – 7 dB gain. However, a noticeable reduction in bandwidth was observed on the proposed antenna array compared with the single patch antenna with is not significant as the focus of the paper is on gain improvement.

Akaninyene et al. [18] proposed the design of two antenna arrays with configurations of 1x2 and 1x4 symmetrical one-dimensional arrangement. The authors employed rectangular geometry on a Roger/RT Duroid substrate with dielectric constant of 2.2 using transmission line model equations with inset feed technique at 2.4 GHz. The results presented by the authors showed a remarkable improvement in antenna gain achieved by the single patch (5.26 dB) to that of the 1x2 antenna array (9.24 dB) and 1x4 antenna array (10.29 dB). However, from observation of the minimum return loss, the proposed antennas' VSWR were above the benchmark value of 2 for the 1x2 and 1x4 antenna arrays which indicates impedance mismatch at the designed frequency.

Sivia et al. [19] proposed a 1x4 triple band rectangular microstrip patch antenna array with operating frequencies between 8 – 12 GHz using Roger/RT Duroid substrate material with dielectric constant of 2.2 and a thickness of 1.6 mm. Sivia et al (year) adopted transmission line model equations with strip line feeding method of design. This was used to compute the dimensions of the patch and the corresponding

feed lines. The results obtained showed that the antenna achieved minimum return losses of -11.8 dB, -12.9 dB and -9.4 dB at 8.86 GHz, 9.16 GHz and 11.01 GHz frequencies, respectively. In terms of gain and directivity, the authors reported gains of 9.95 dB, 10.76 dB and 7.97 dB with directivities of 13.11 dB, 12.65 dB and 11.25 dB at corresponding frequencies of 8.86 GHz, 9.16 GHz and 11.01 GHz frequencies. A rule of thumb in microstrip antenna design is to achieve a VSWR below 2 and a minimum return loss that is below -10 dB mark as proof of effective impedance match at exact or approximately the designed frequency. From observation, the proposed antenna fell short of meeting the desired triple band as outlined from their objective.

3. METHODOLOGY

This section presents the design steps for single band RMSA at 2.4 GHz followed by the considerations for the design of multi-element antenna arrays proposed.

3.1 Single Band Patch Antenna Design

The proposed antennas have basic rectangular patch shapes, FR-4 substrate with a dielectric constant (ϵ_r) = 4.2, loss tangent ($\tan\delta$) = 0.019 and resonant frequency (f_r) = 2.4 GHz, respectively. The height (h) of the substrate is determined from Equations (1) and (2) as:

$$h \leq 0.3 \times \frac{\lambda_0}{2\pi\sqrt{\epsilon_r}} \quad (1)$$

$$\lambda_0 = \frac{c}{f_r} \quad (2)$$

A single band microstrip antenna with centre frequency of 2.4 GHz is first designed using transmission line model equations obtained from [10,20,21]. The rectangular patch structure acts as a resonator; thus, the length and width of the patch are typically selected in such a way that $L_p < W_p < 2L_p$ for efficient and enhanced radiation. The design equations used for the rectangular microstrip patch are itemized as follows:

- i) The width (W_p) of the microstrip patch is computed from Equation 3.

$$W_p = \frac{c}{2f_r\sqrt{\frac{\epsilon_r+1}{2}}} \quad (3)$$

- ii) The effective dielectric constant (ϵ_{reff}) is obtained from Equation 4.

$$\epsilon_{\text{reff}} = \frac{\epsilon_r+1}{2} + \frac{\epsilon_r-1}{2} \left[1 + 12 \left(\frac{h}{W_p} \right) \right]^{-1/2} \quad (4)$$

- iii) The effective length L_{eff} of the patch is calculated from Equation 5.

$$L_{\text{eff}} = \frac{c}{2f_r \sqrt{\epsilon_{\text{reff}}}} \quad (5)$$

- iv) The length extension (ΔL) is deducted from the length of the patch (L_p) with actual length of the patch unchanged (in most cases). The length extension is considered due to fringing field as seen in Equation 6.

$$\Delta L = 0.412h \frac{[\epsilon_{\text{reff}}+0.3] \left[\frac{W}{h} + 0.264 \right]}{[\epsilon_{\text{reff}}-0.258] \left[\frac{W}{h} + 0.813 \right]} \quad (6)$$

- v) Calculation of actual length of patch (L_p) is done using Equation 7.

$$L_{\text{eff}} = L_p + 2\Delta \quad (7)$$

$$L_p = L_{\text{eff}} - 2\Delta \quad (8)$$

- vi) Calculation of the ground plane dimensions (L_g and W_g): A major assumption adopted by the transmission line model is the use of infinite ground planes for simplified analysis. However, it is essential to have a finite ground plane for practical contemplations. For both finite and infinite ground planes, the size of the ground plane must be greater than the patch dimensions by approximately six times the substrate thickness (h) all around the patch periphery [10,22]. Hence, for this design, the ground plane dimensions are calculated thus:

$$L_g = L_p + 6h \quad (9)$$

$$W_g = W_p + 6h \quad (10)$$

Determination of the patch thickness (t): The metallic patch is selected to be very thin such that $t \ll \lambda_0$. Similar to the feed configurations outlined by [23], inset and quarter wave feeding methods are used in this study for different antenna designs.

The quarter-wave feedline dimensions are determined from the Equations 11 to 16. The

conductance of a single slot of finite width is given by [10,24] as follows.

$$G = \frac{W}{120 \lambda_0} \left[1 - \frac{(k_0 h)^2}{24} \right] \text{ for } \frac{h}{\lambda_0} < \frac{1}{10} \quad (11)$$

$$B = \frac{W}{120 \lambda_0} [1 - 0.636 \ln(k_0 h)^2] \text{ for } \frac{h}{\lambda_0} < \frac{1}{10} \quad (12)$$

where λ_0 is the free space wavelength and k_0 is the wave number hence;

$$k_0 = \frac{2\pi}{\lambda_0} \quad (13)$$

The input conductance of the patch fed on the edge is noted to be twice the conductance of one of the edge slots. This can be obtained by using Equation 14 as stated in [25] as:

$$R_{\text{in}} = \frac{1}{2G} \quad (14)$$

If the input edge impedance of the antenna is R_{in} , the characteristic impedance of the quarter wave transmission line (QWT) is given [10,25] as:

$$Z_1 = \sqrt{Z_0 R_{\text{in}}} \quad (15)$$

The width of the quarter-wave feed line is computed using the mathematical expression given in [10,26,27] as follows:

$$\frac{W_Q}{h} = \begin{cases} \frac{9e^A}{e^{2A}-2} & \text{for } \frac{W_Q}{h} < 2 \\ \frac{2}{\pi} \left[B - 1 - \ln \left((2B-1) + \left(\frac{\epsilon_r-1}{2\epsilon_r} \right) \left\{ \ln(B-1) + 0.39 - \frac{0.61}{\epsilon_r} \right\} \right) \right] & \text{for } \frac{W_Q}{h} > 2 \end{cases} \quad (16)$$

where;

$$A = \frac{Z}{60} \sqrt{\frac{\epsilon_r+1}{2} + \frac{\epsilon_r-1}{\epsilon_r+1}} \left(0.23 + \frac{0.11}{\epsilon_r} \right) \quad (17)$$

$$B = \frac{377\pi}{2Z\sqrt{\epsilon_r}} \quad (18)$$

Length of the quarter-wave feedline is computed using Equation 19.

$$L_Q = \frac{\lambda}{4} = \frac{\lambda_0}{4\sqrt{\epsilon_{\text{reff}}}} \quad (19)$$

The schematic diagram of the quarter-wave feed single band microstrip antenna showing designed parameters is presented in Fig.1.

The summary of the dimensions of the single patch antenna designed at 2.4 GHz are presented in Table 1.

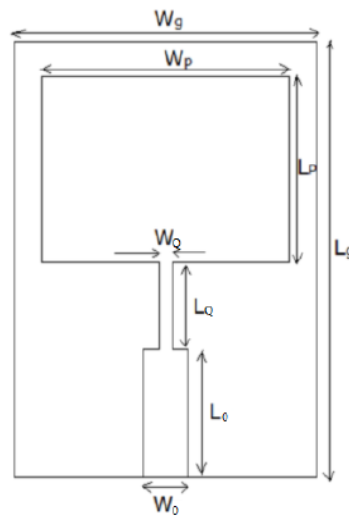


Fig. 1. Schematic diagram of MSA using quarter-wave feed at 2.4 GHz

Table 1. Design dimensions of 2.4 GHz single band edge-fed RMSA

Design Parameter	Values
Patch dimensions:	
Length (L_p)	29.52 mm
Width (W_p)	37.97 mm
Dielectric constant (ϵ_r)	4.2
Substrate height (h)	1.60 mm
Patch thickness (t)	0.20 mm
Ground plane dimensions:	
Length of ground plane (L_g)	39.12 mm
Width of ground plane (W_g)	47.57 mm
Feed line dimensions:	
Width of quarter wave feed section (W_Q)	0.83 mm
Width of 50 Ω transmission line (W_0)	3.17 mm
Length of 50 Ω transmission line (L_0)	7.00 mm
Length of quarter wave feed line (L_Q)	15.44 mm
Input edge impedance of the patch (R_{in})	185.19 Ω
Characteristic impedance of the feed line (Z_0)	50 Ω
Characteristic impedance of quarter wave transformer (Z_1)	96.23 Ω

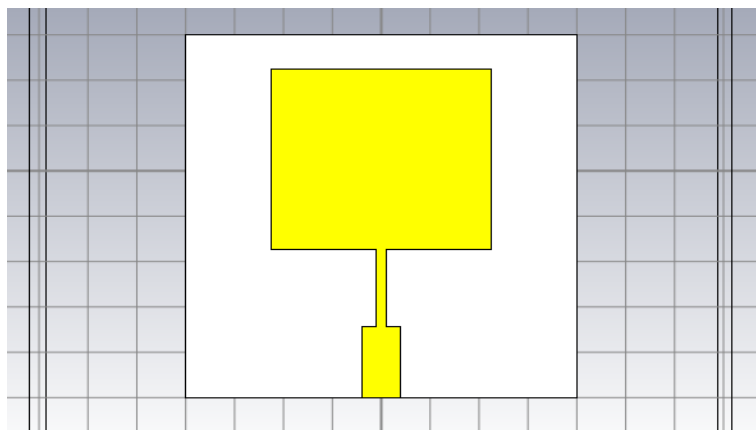


Fig. 2. Model of quarter wave-fed MSA at 2.4 GHz using CST Studio

3.2 Series-fed 1 x 4 MSA Array Design

A general assumption by most authors who worked on this configuration according to [28], is that, since the microstrip patch is fed mainly by a 50Ω feed, the feed line emanating from feeding patch should equally maintain the same width transformed from previously used quarter-wave line for the receiving patch.

Therefore; $W_Q = 0.83 \text{ mm}$

However, as stated by [8], to lower the risk of mutual coupling, maintain single mode propagation among radiating elements and to have in-phase array elements and radiation in

normal direction, the distance between array elements is taken to be about half wavelength $\left(\frac{\lambda_{air}}{2}\right)$; thus

$$\text{patch spacing, } d = \frac{\lambda_{air}}{2} = \frac{122}{2} = 61 \text{ mm}$$

Another notable reason why a good separation distance d , is maintained is to lower the risk of mutual coupling between radiating element and to allow for single mode propagation among radiating elements. The Schematic diagram of 1 x 4 microstrip antenna array is presented in Fig. 3.

The simulated series-fed 1 x 4 antenna array in CST Studio is presented in Fig. 4.

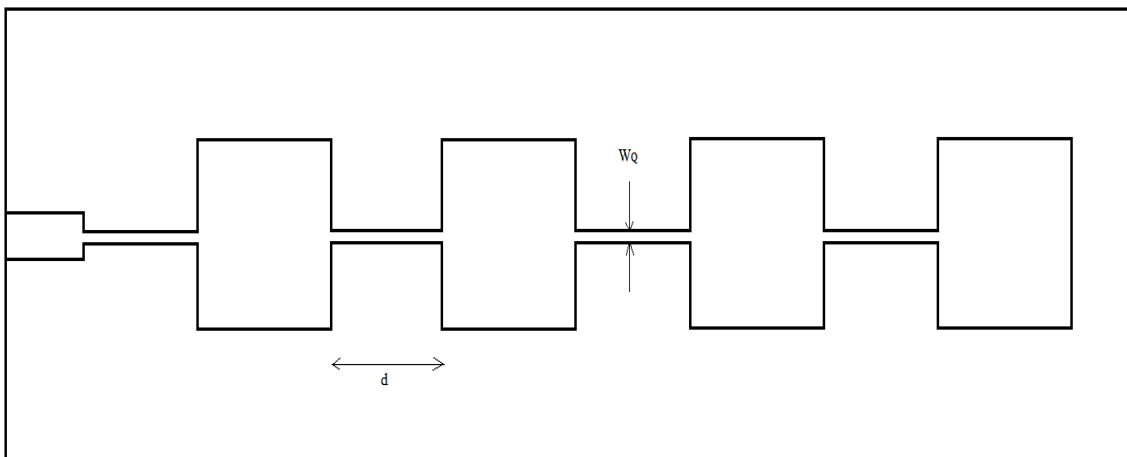


Fig. 3. Schematic diagram of series-fed 1 x 4 patch antenna array

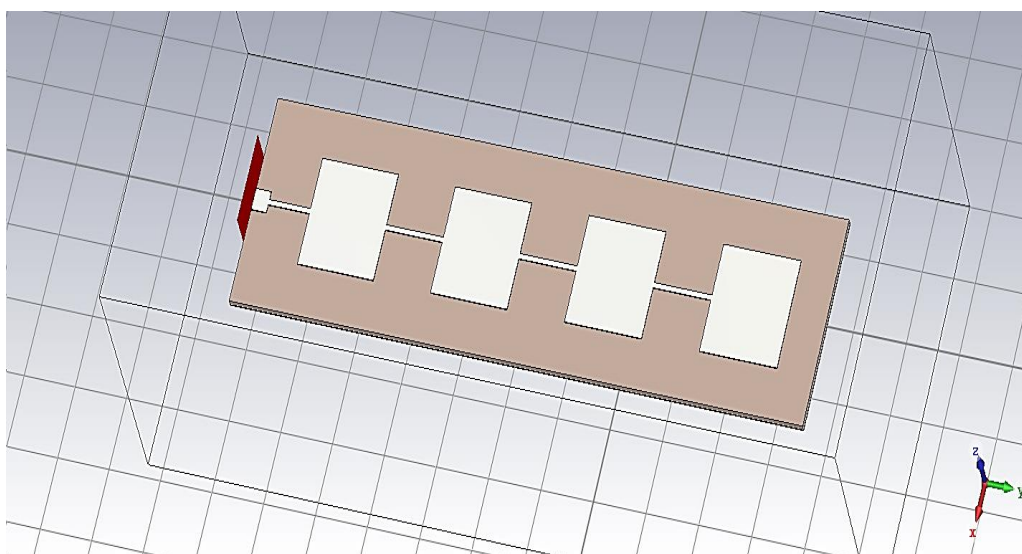


Fig. 4. Model of series-fed 1 x 4 patch MSA array

3.3 Cooperate-fed MSA Array Design

The cooperate-series-fed 2 x 2 MSA antenna array proposed in this study comprises two primary patches and two secondary patches. The primary patches are patches that are directly linked to the feed network, while the secondary patches are those that are fed directly from the primary patches.

To reduce the complexity of the feeding network of the proposed cooperate-series-fed 2 x 2 MSA array, inset-fed technique is adopted for the primary patches using available computational formulas to determine the dimensions of the feed network, hence the need for another design configuration as itemized in the following steps:

Step 1: Calculate the notch width, g using the equation from [29] as given in Equation 20.

$$g = \frac{c f_r \times 10^{-9} \times 4.65 \times 10^{-9}}{\sqrt{2\epsilon_{\text{reff}}}} \quad (20)$$

Step 2: Calculate the resonant input resistance R_{in} thus;

$$R_{\text{in}}(y = y_0) = \frac{1}{2(G_1 + G_{12})} \cos^2\left(\frac{\pi y_0}{L_p}\right) \quad (21)$$

The equation for the characteristic impedance Z_0 is given as;

$$Z_0 = \begin{cases} \frac{60}{\sqrt{\epsilon_{\text{reff}}}} \ln\left[\frac{8h}{W_f} + \frac{W_f}{4h}\right] & \text{for } \frac{W_f}{h} \leq 1 \\ \frac{120\pi}{\sqrt{\epsilon_{\text{reff}}}} \left[\frac{W_f}{h} + 1.393 + 0.667 \ln\left(\frac{W_f}{h} + 1.444\right) \right] & \text{for } \frac{W_f}{h} \geq 1 \end{cases} \quad (22)$$

$$I_1 = -2 + \cos(X) + X S_i(X) + \frac{\sin(X)}{X} \quad (23)$$

$$X = kW_p \quad (24)$$

$$G_1 = \frac{I_1}{120\pi^2} \quad (25)$$

$$G_{12} = \frac{1}{120\pi^2} \int_0^\pi \left[\frac{\sin\left(\frac{kW_p}{2} \cos\theta\right)}{\cos\theta} \right]^2 J_0(kL_p \sin\theta) \sin^3\theta d\theta \quad (26)$$

where J_0 is the Bessel function of the first kind of order zero. G_{12} is resolved using MATLAB-based program developed for the calculation of rectangular microstrip antenna parameters.

Step 3: Calculate the inset feed recessed distance y_0 and the width of the transmission line W_f thus;

$$Z_0 = R_{\text{in(edge)}} \cos^2\left(\frac{\pi}{L_p} y_0\right) \quad (27)$$

$$y_0 = \frac{L_p}{\pi} \cos^{-1} \left[\sqrt{\frac{Z_0}{R_{\text{in(edge)}}}} \right] \quad (28)$$

According to [26], the width of the transmission line is calculated thus, for $\frac{W_f}{h} > 2$, Equation 16 was used. The summary of the inset feed dimensions computed is presented in Table 2. Note that the patch dimensions were omitted in the table because it was already presented in Table 1.

Table 2. Feed dimensions of 2.4 GHz single band inset-fed RMSA

Parameter	Value (mm)
Width of transmission line, W_f	3.30
Inset fed gap, g	1.20
Inset fed distance, y_0	11.12
Length of 50 Ω line, L_f	4.80

The schematic diagram of the designed 2.4 GHz inset-fed antenna is depicted in Fig. 6

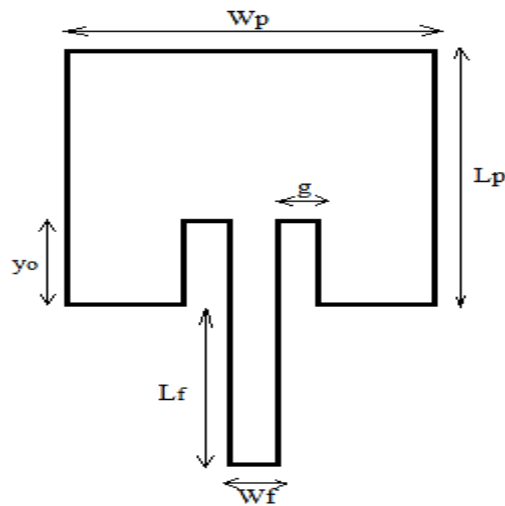


Fig. 5. Schematic diagram of inset-fed MSA at 2.4 GHz

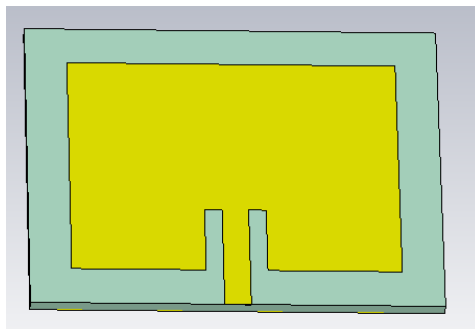


Fig. 6. Model of 2.4 GHz inset-fed Single Band MSA in CST studio

The proposed array configuration is principally comprised of four rectangular microstrip patch antennas with two feeding methods for the primary and secondary patches. The corporate feed network was used for transmission and collection of power for the primary patches while series feed was employed for the secondary patches. Typical corporate feed network is subdivided into three parts:

- i. Microstrip Lines
- ii. Microstrip T-Junctions power divider
- iii. Mitred Bends

i. Microstrip Lines: A microstrip line feed of $Z_0 = 50 \Omega$ ramose off into two feed lines of $2Z_0$ ($Z_1 = 2 \times 50 = 100 \Omega$) capacity which further branches into a $Z_2 = 70.7 \Omega$ feed line as expressed in Equation 15 is used for in a parallel array feed network for the proposed antenna.

$$Z_3 = \sqrt{50 \times 100} = 70.7 \Omega$$

In the feed network, three different impedance transmission lines (50 , 70.7 and 100Ω) were used. All the elements of the array are matched to the standard 50Ω impedance and hence the width of 50Ω was calculated earlier as $W_0 = 3.20$ mm. Width of 70.7Ω and 100Ω line are computed using Equations 17 and 18 where $Z = 70.7$ or 100Ω , $\epsilon_r = 4.2$, $h = 1.6$ mm.

Width of 70.7Ω therefore is computed with $A = 2.06$ as $W_3 = 1.05$ mm.

Width of 100Ω therefore is computed with $A = 2.85$ as $W_2 = 0.50$ mm.

The length of the quarter-wave line was previously calculated as 15.40 mm. It important to emphasize as highlighted by [10] that the length of the transmission has little or no significant effect on the performance of the antenna. Hence, an appropriate length was selected throughout the design of the antenna.

ii Microstrip T- junction power divider: The T-Junction power divider/splitter is a three port network similar to Wilkinson 3 port power divider but it does not have any isolation between the output ports [30]. In Wilkinson power divider, the output ports 2 and 3 have an isolation from each other. The resistance applied between port 2 and 3 is used to stop the power from transmitting in the backward direction towards the source. Usually the reflection affects the VSWR, but in case of T-Junction, it is still acceptable because of the quarter wavelength length between the two output ports, which somehow cancel the reflection at the input as illustrated in Fig. 7

P_1 is the input port with an impedance of $Z_1 = Z_0$ and a width of $W_1 = W_f$. The power at P_1 is split into two outputs, $2P_2$. T-junction strongly depends upon the quarter wavelength of the output port, for the smooth transition of power from high impedance to low impedance microstrip lines. Z_1 is the impedance of the common port, while Z_2 is the impedance of split ports. Mathematically Z_2 is given by Equation 29;

$$Z_2 = 2 \times Z_1 \tag{29}$$

iii Mitred Bend: In notable cases of the parallel feed networks, unlike array series feed networks, the transmission lines are not always in a straight line, they are made to bend up to certain degrees. For instance, if a horizontal transmission line has to be bent to a vertical transmission line by a 90° change in direction, [16] stated that this results in most of the power from the input being reflected back at the discontinuity towards the source, which reduces the performance of the system. A 90° bend in transmission line causes a change in capacitance of the line, which in turn changes the impedance of the line. The change in impedance causes a mismatch with the input port impedance. To resolve this problem, microstrip mitred bends are introduced. The purpose of the mitred bend is to chop that little amount of capacitance to bring back the impedance of the line to the matching impedance. A mitred bend is illustrated in Fig. 8.

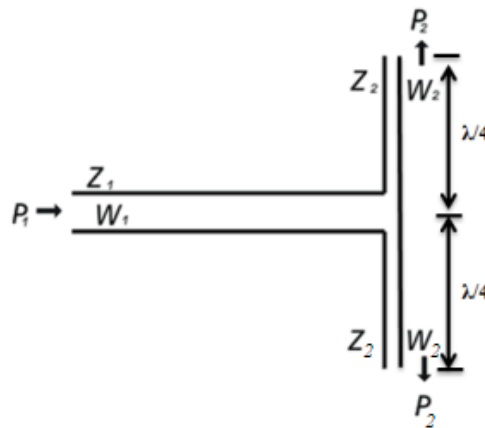


Fig. 7. Microstrip T-junction

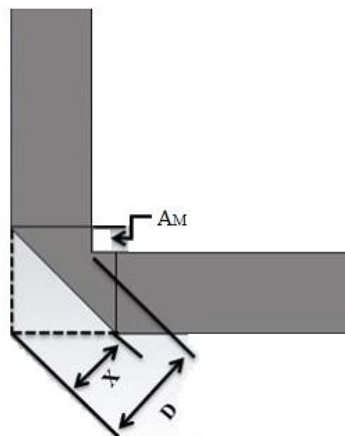


Fig. 8. Microstrip mitred bend

Expressions for A_M , X and D are given by Equations 3.30 to 3.32 as:

$$D = W \times \sqrt{2} \tag{30}$$

where W is the width of the transmission line and h is the height of the substrate. Only the input 50 Ω line will incorporate the bend in the 1 x 4 array antenna design, $W = 3.30$ mm.

$$X = D \times \left[0.52 + 0.65e^{\left(-1.35\frac{W}{h}\right)} \right] \tag{31}$$

$$A_m = \left(X - \frac{D}{2} \right) \times \sqrt{2} \tag{32}$$

Table 3 gives a summary of the computed dimensions of patch and feed network of the proposed array antennas.

For ease of understanding, it is important to start by first designing a 1 x 2 MSA array at 2.4 GHz which served as a building block for both the 1 x

4 cooperate-fed antenna array and the 2 x 2 cooperate-series-fed antenna array.

The feed network design for the 1 x 2 array antenna starts with a 50 Ω line branching off to a 100 Ω feed that is further transformed to a 70.71 Ω before the final branch that feeds the patch with suitable impedance match as illustrated in the sketch showing the width corresponding to each impedance in Fig. 8. The only difference between 1 x 2 feed network and that of 1 x 4 cooperate feed is that in the cooperate-fed 1 x 2, the final feed stage of the cooperate feed (50 Ω) is repeated to achieve a 4-element configuration as given in the schematic diagram of Fig. 9.

Figs. 10 and 11 gives the model of the 1 x 2 and 1 x 4 MSA antenna array designed in CST Studio.

The model of designed antennas in CST studio is presented in Figs. 10 to 12

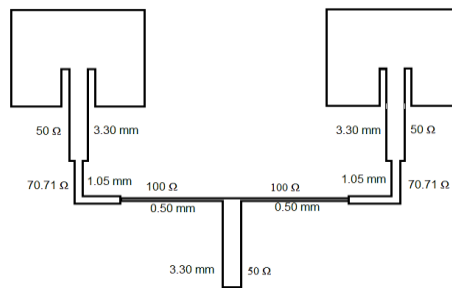


Fig. 9. Schematic Diagram of Cooperate-fed 1 x 2 Antenna Array

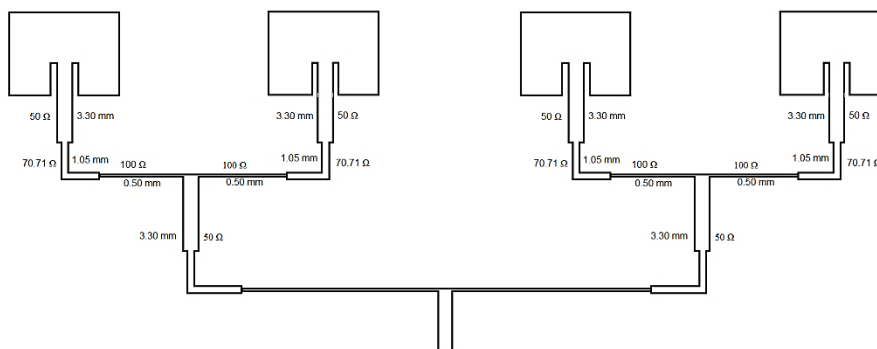


Fig. 10. Schematic Diagram of Cooperate-fed 1 x 4 Antenna Array

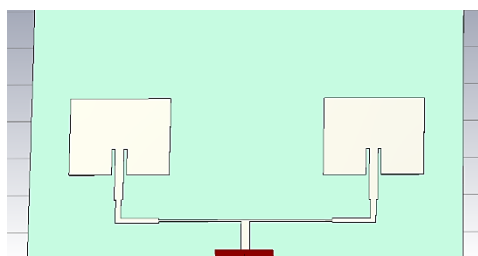


Fig. 11. Model of 1 x 2 Cooperate-fed MSA Array

Table 3. Proposed 2 x 2 cooperate-series-fed MSA array dimensions

Parameter	Value (mm)
Patch dimensions:	
Length of patch, L_p	27.52
Width of patch, W_p	39.97
Dielectric constant, ϵ_r	4.2
Height of substrate, h	1.60
Feed dimensions:	
Width of 50 Ω transmission line, W_f	3.30
Width of 70.7 Ω transmission line, W_3	1.05
Width of 100 Ω transmission line, W_2	0.50
Inset distance, y_o	11.12
Inset gap, g	1.20
Length of transmission line, L_f	4.80
Length of quarter wave, L_q	14.90
Resonance Frequency, f_r	2.4 GHz
Ground plain dimensions:	
Length of ground plain, L_g	70
Width of ground plan, W_g	160
Mitred bend dimensions:	
A_m	0.40
X	2.62
D	4.67
Distance between Patches, d	61.00

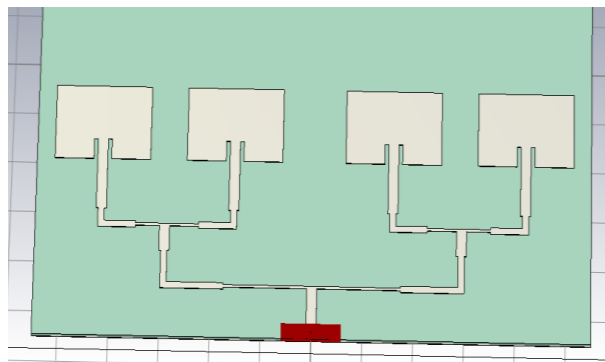


Fig. 12. Model 1 x 4 Cooperate-fed MSA Array

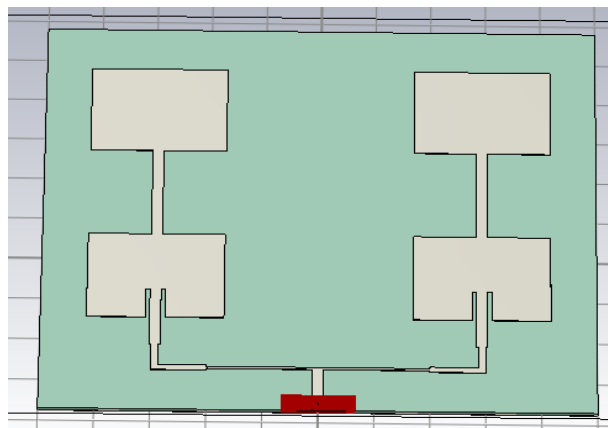


Fig. 13. Model of 2 x 2 Cooperate-series-fed 2 x 2 MSA Array

4. RESULTS AND DISCUSSION

The results and performance analysis of all antennas designed in section 3 are presented in this section. Results are presented in polar, two-dimensional (2-D) and three-dimensional (3-D) plots. Antenna parameters such as return loss, bandwidth, VSWR, directivity and gain were used to assess the proposed antennas' performance.

4.1 Return loss

Figs. 13 to 17 gives the return loss plot the single band antenna and the multi-element antennas considered. From Fig. 13, a minimum return loss of -19.8034 dB at a resonant frequency of 2.4 GHz along with impedance bandwidth of 65.3 MHz was achieved by the single band quarter-wave-fed RMSA. The 1×4 RMSA array showed

a minimum return loss of -12.933 dB resulting in an impedance bandwidth of 152.07 MHz as depicted in Fig. 14.

A minimum return loss of -26.394 dB at resonance frequency of 2.416 GHz and an impedance bandwidth of 68.3 MHz was achieved by the inset-fed single band antenna as given in Fig. 15. The return loss plots of the 1×2 and 1×4 cooperate-fed antenna array are presented in Figures 16 and 17 from which minimum return loss of -22.901 dB and -31.898 dB at 2.368 GHz and 2.395 GHz resonance frequencies were achieved. Also, impedance bandwidth of 33.06 MHz and 44.33 MHz, respectively were achieved. Furthermore, a minimum return loss of -37.83 dB at 2.407 GHz was achieved by the proposed 2×2 cooperate-series-fed array antenna along with impedance bandwidth of 50.41 MHz as illustrated in Fig. 18.

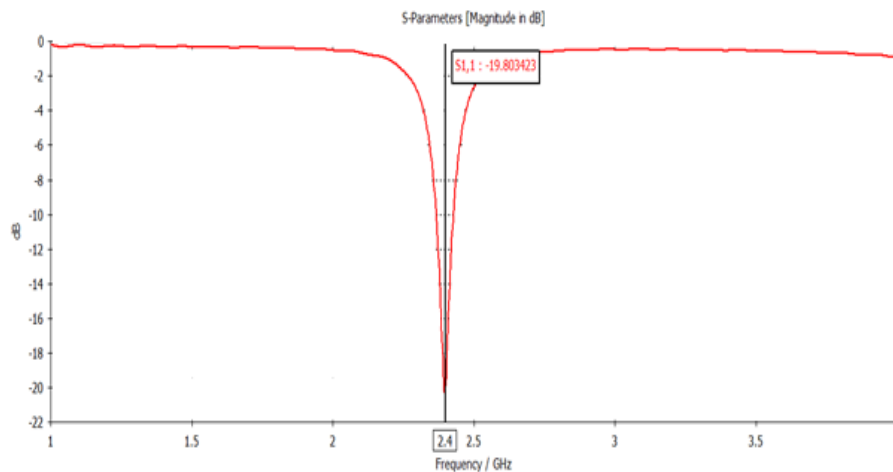


Fig. 14. Return Loss plot of the quarter-wave-fed single-band antenna at 2.4 GHz

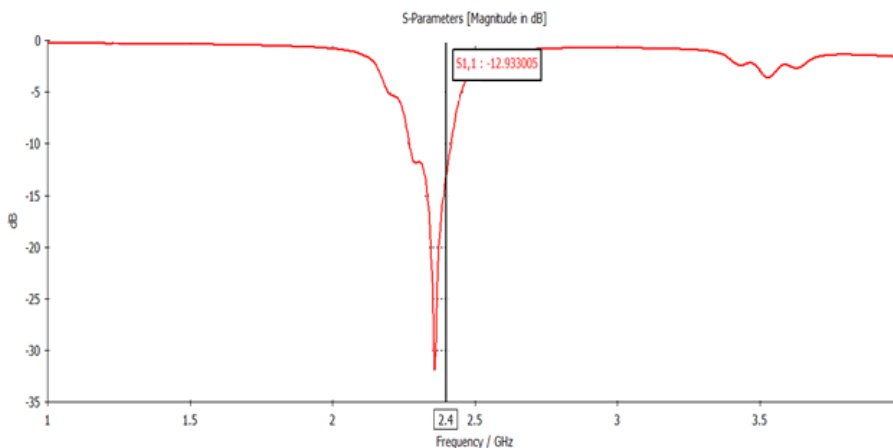


Fig. 15. Return Loss plot of 1×4 series-fed antenna array at 2.4 GHz

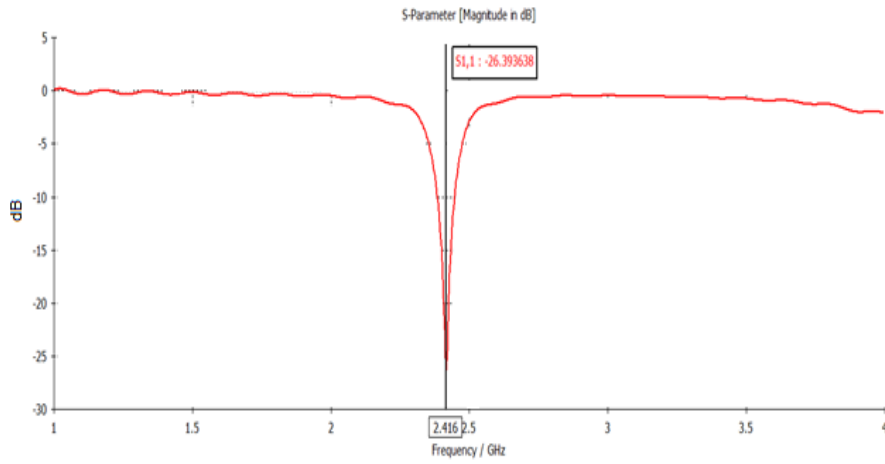


Fig. 16. Return Loss plot of inset-fed single band antenna

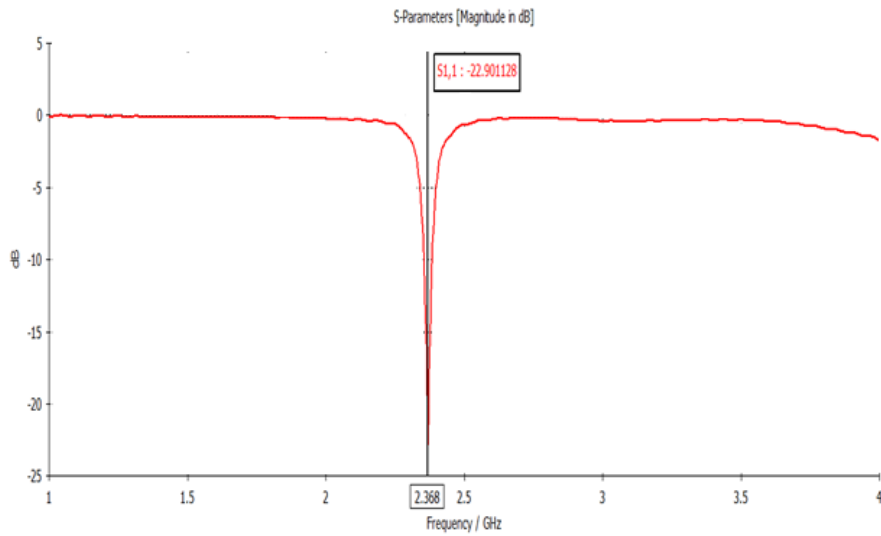


Fig. 17. Return loss plot of the proposed 1 x 2 cooperate-fed antenna array

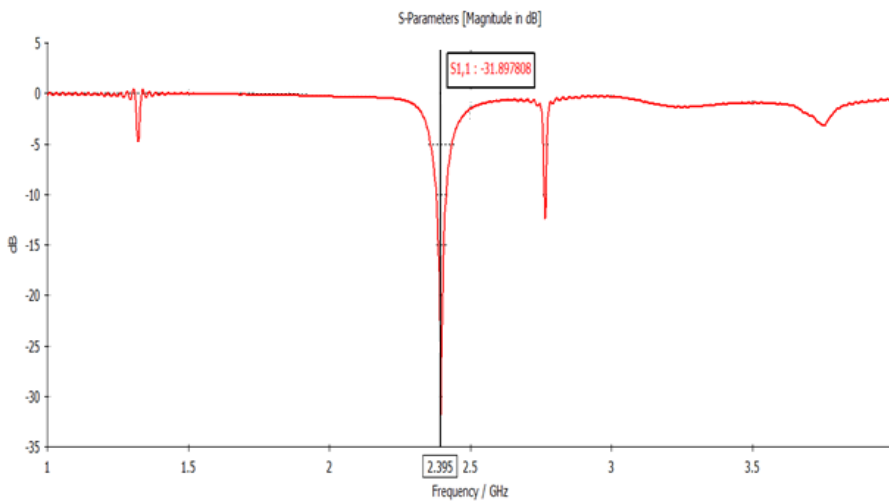


Fig. 18. Return loss plot of the proposed 1 x 4 cooperate-fed antenna array

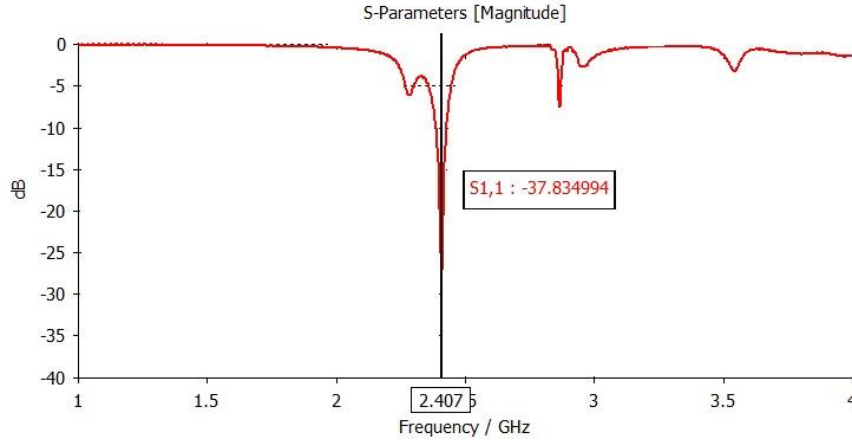


Fig. 19. Return loss plot of the proposed 2 × 2 cooperate-series-fed antenna array

Thus, the percentage impedance bandwidth of the antennas considered are presented as follows:

Using Equation (33) from [1], [31], the percentage bandwidth at 2.4 GHz of the antennas designed were calculated thus;

$$\% \text{ bandwidth} = \frac{f_H - f_L}{f_C} \times 100 \quad (33)$$

QWT-fed single band antenna - Bandwidth =

$$\frac{2.4322 - 2.3669}{2.4} \times 100 = 2.72 \%$$

1 x 4 series-fed antenna array – Bandwidth =

$$\frac{2.4198 - 2.2678}{2.4} \times 100 = 6.34\%$$

Inset-fed single band Bandwidth =

$$\frac{2.4512 - 2.3829}{2.4} \times 100\% = 2.85$$

1 x 2 cooperate-fed array antenna - Bandwidth =

$$\frac{2.3876 - 2.3545}{2.4} \times 100 = 1.38 \%$$

1 x 4 cooperate-fed array antenna - Bandwidth =

$$\frac{2.4187 - 2.3744}{2.4} \times 100 = 1.85 \%$$

2 x 2 cooperate-series-fed array antenna -

$$\text{Bandwidth} = \frac{2.4322 - 2.3818}{2.4} \times 100 = 2.26 \%$$

The percentage bandwidths obtained from the return loss plots gives an interesting trend observed from the calculated values in that, a noticeable drop in bandwidth was noticeable in the arrays using cooperate-feed network compared to the series-feed with exception of the combined-feed (hybrid-feed) that showed an improvement in bandwidth. However, in all the

designs, the percentage bandwidth of the series-fed 1 × 4 array antenna was higher than that of the counterpart arrays and the single band antennas.

Fig. 20 gives a combined s-parameter plot of all array antennas from where it is seen that the 2 × 2 hybrid-fed MSA array achieved the highest minimum return loss of -37.83 dB.

4.2 Directivity of Designed Antennas

All six designed antenna radiation patterns are on the broadside. Fig. 21 shows the H-plane ($\varphi = 90^\circ$) directivity of the single band antennas at 2.4 GHz, having a main lobe magnitude of 6.24 dBi and 6.09 dBi and a main lobe direction of 8° and 3° , respectively. Half power beamwidth (HPBW) of 97.9° and 97.2° was equally obtained. These results clearly show a good performance of the simulated single-band antenna having nearly an omnidirectional radiation pattern with side lobe levels of 0 and -13.6 dB at 2.4 GHz.

The H-plane ($\varphi = 90^\circ$) directivity of the proposed 1 × 4 series-fed and 1 × 4 cooperate-fed is illustrated in Fig. 22. Main lobe magnitudes of 10.5 dBi and 11.6 dBi and main lobe directions of 17° and 46° , with a HPBW of 29.2° and 43.5° , respectively. Corresponding side lobe levels of -8.8 dB and -1.6 dB were observed from the directivity polar plot.

The H-plane ($\varphi = 90^\circ$) directivity of the 1 × 2 cooperate-fed and 2 × 2 cooperate-series-fed RMSA arrays are shown in Fig. 23; it can be seen that there is a slight increment in the main lobe magnitude (10.1 dBi and 14.1 dBi). Side lobe level, however, increased (-13.4 dB and -12.4 dB) in comparison with the single band patches (Fig. 21) and the arrays of Fig. 20.

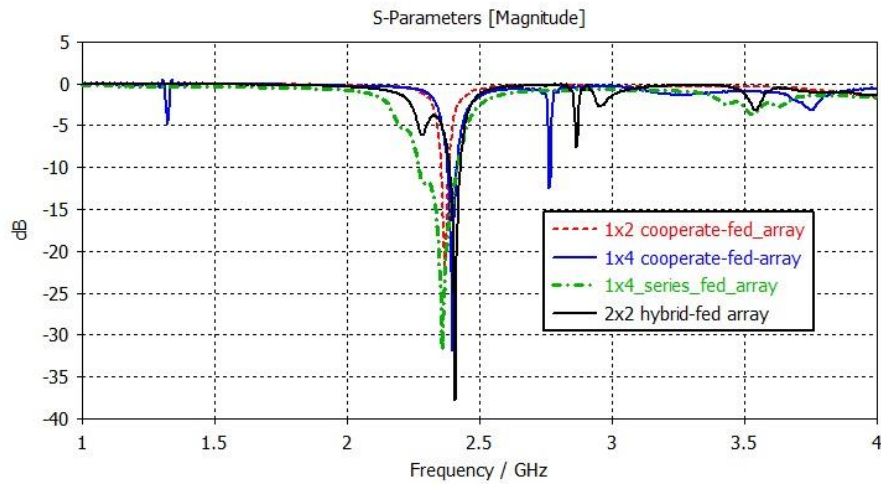


Fig. 20. Comparison of array antennas s-parameters

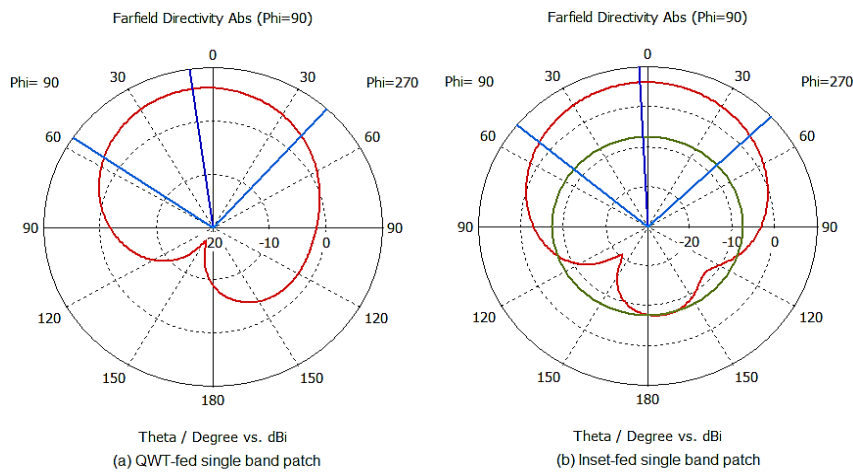


Fig. 21. Directivity of single band antennas at 2.4 GHz in H-plane ($\phi = 90^\circ$)

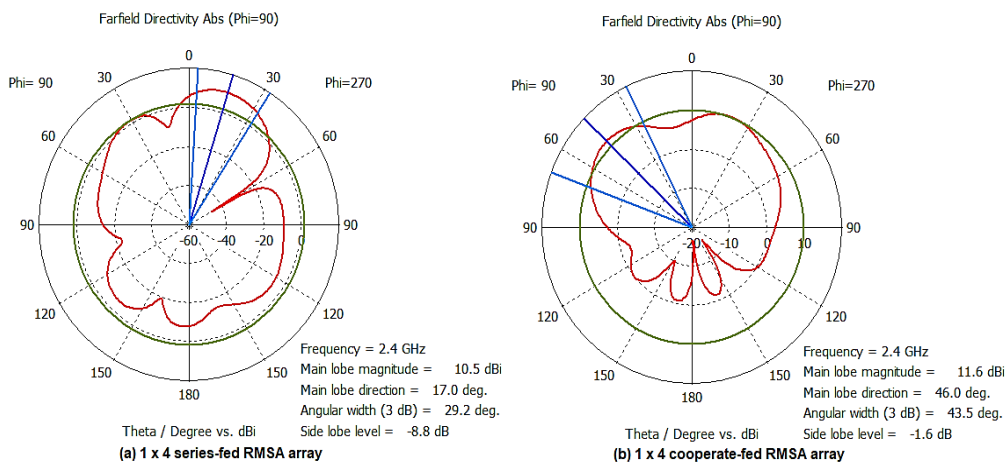


Fig. 22. Directivity of proposed antenna arrays at 2.4 GHz in H-plane ($\phi = 90^\circ$)

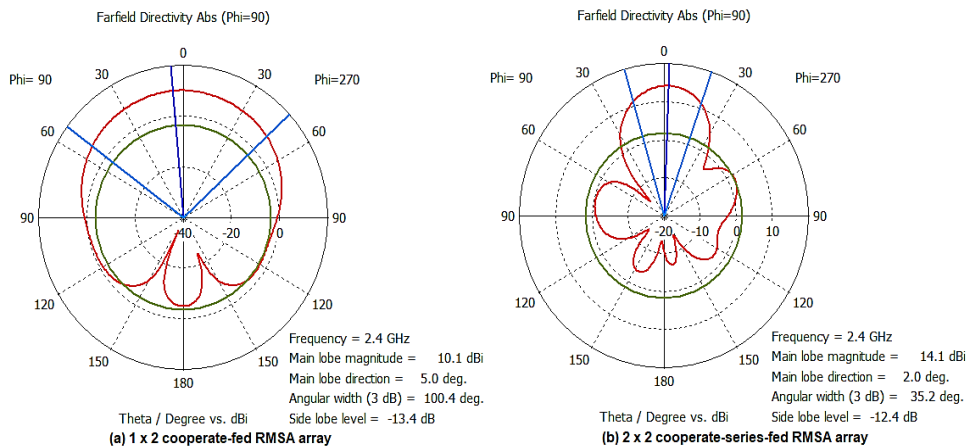


Fig. 23. Directivity of proposed antenna arrays at 2.4 GHz in H-plane ($\phi = 90^\circ$)

The E-plane ($\phi = 0^\circ$) directivity of the single patches is given in Fig. 24. A slight decrement in the main lobe magnitude (6.16 dBi from 6.24 dBi and 6.08 dBi from 6.09 dBi) was observed. The main lobe direction remained consistent at 0° in both designs better than the variation obtained in the H-plane; the HPBW of both antennas was above 90° . Main lobe magnitudes of 5.68 dBi and 7.39 dBi and HPBW of 95.3° and 26.2° were obtained by the 1×4 series-fed and 1×4 cooperate-fed RMSA arrays with side lobe levels of -14 dB and -9.3 dB, respectively as presented in Fig. 25.

Fig. 26 gives the directivity polar plot in the E-plane of the 1×2 cooperate-fed and 2×2 cooperate-series-fed RMSA arrays. Both antennas were designed at 2.4 GHz with the 1×2 array resonating with a maximum magnitude of 10 dBi with HPBW of 28.4° and a side lobe level of -8.0 dB while the 2×2 array

achieved a maximum magnitude of 14.1 dBi with HPBW of 28.4° and a side lobe level of -8.4 dB.

4.3 Efficiency and Gain of the Proposed Antenna

Fig. 27 gives the combined radiation efficiency plot of all array antennas considered in this study. From Fig. 26, 1×2 parallel-fed MSA array achieved a radiation efficiency of about 99% while the 1×4 series fed MSA array achieved a radiation efficiency of 86%. The 2×2 MSA array with hybrid fed showed a radiation efficiency of 89% while the 1×4 parallel fed MSA array achieved 98% efficiency.

The IEEE 3-D gain of the two single band antennas (QWT-fed and Inset-fed) designed in section 3 are shown in Fig. 28. The patches achieved gains of 3.47 dB and 4.85 dB at 2.4 GHz.

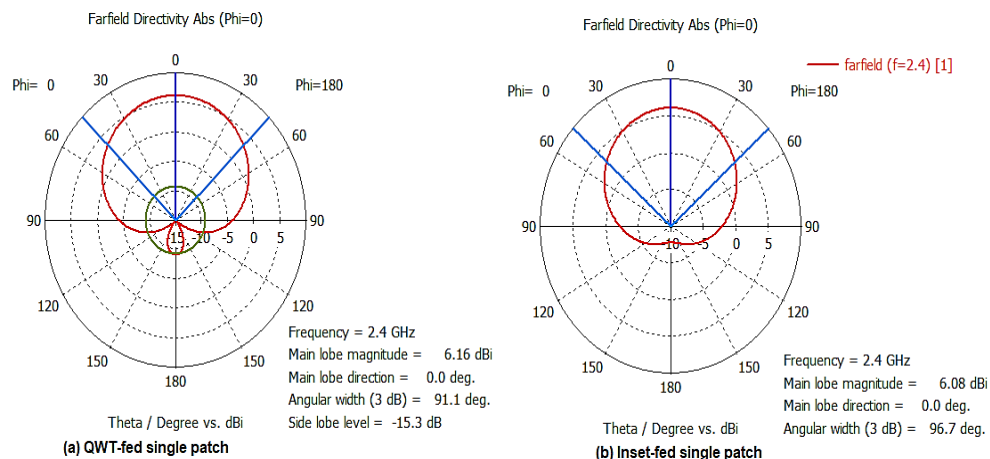


Fig. 24. Directivity of single band antenna at 2.4 GHz in E-plane ($\phi = 0^\circ$)

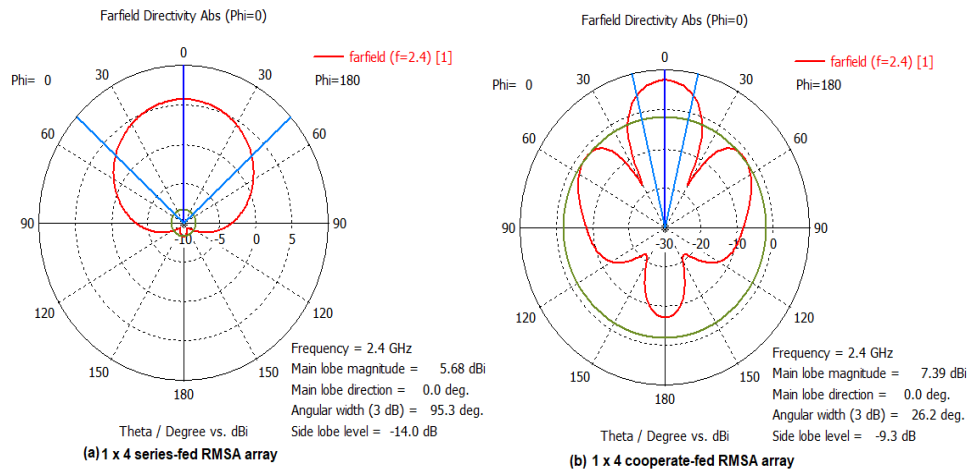


Fig. 25. Directivity of array antennas at 2.4 GHz in E-plane ($\phi = 0^\circ$)

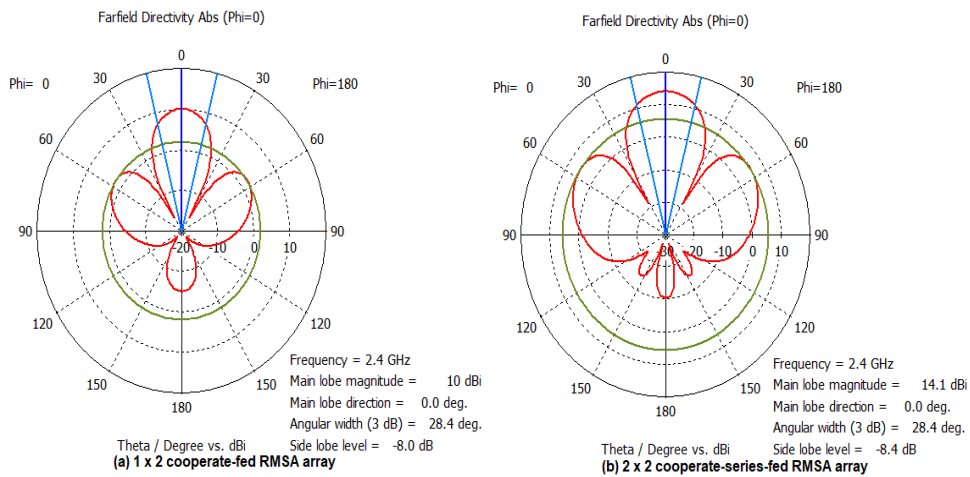


Fig. 26. Directivity of array antennas at 2.4 GHz in E-plane ($\phi = 0^\circ$)

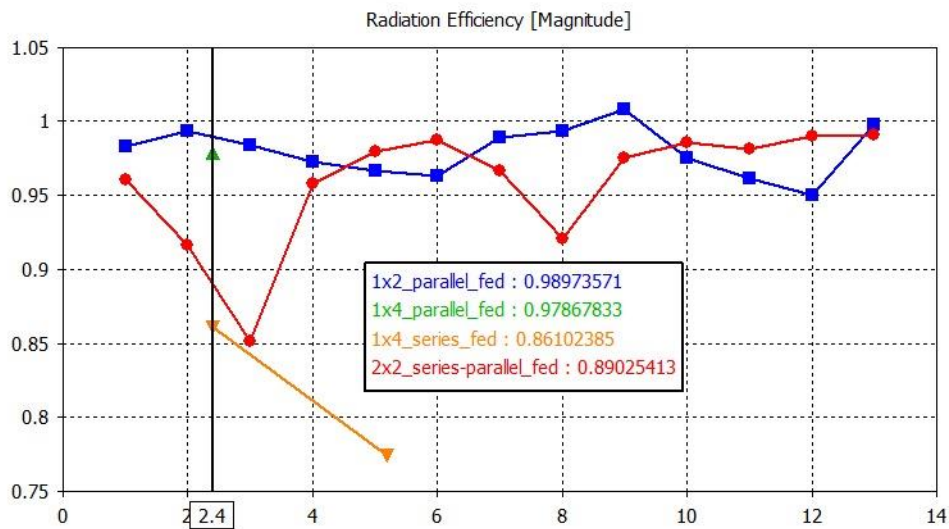


Fig. 27. Radiation efficiency of array antennas at 2.4 GHz

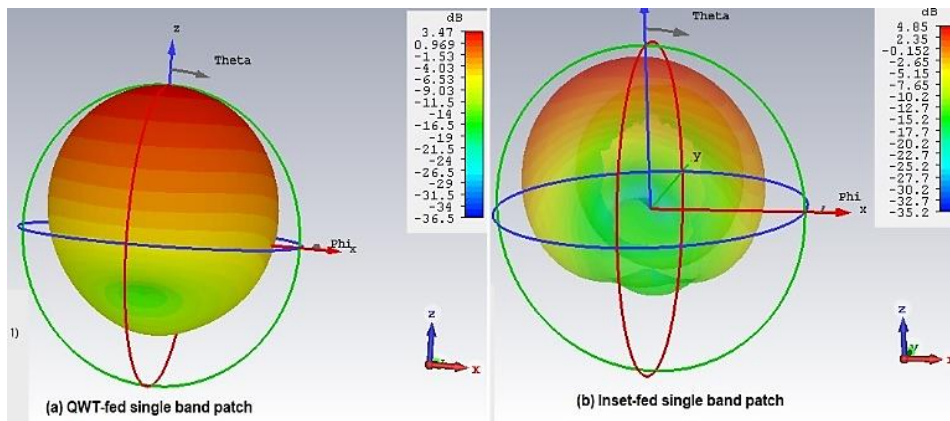


Fig. 28. 3-D gain of single band antenna at 2.4 GHz

The standard IEEE gain of the 1×4 series-fed and 1×4 cooperate-fed RMSA arrays is shown in Fig. 29. Gains of 5.06 dB and 11.50 dB were respectively achieved at 2.4 GHz.

The gains of the 1×2 cooperate-fed and 2×2 cooperate-series-fed RMSA arrays are presented

in Fig. 30. While the 1×2 cooperate-fed array achieved a gain of 10.1 dB, a significant improvement from the single band patches earlier designed, the 2×2 hybrid-fed array showed a slightly superior gain performance of 14 dB and also quite higher than that achieved by 1×4 cooperate-fed antenna array.

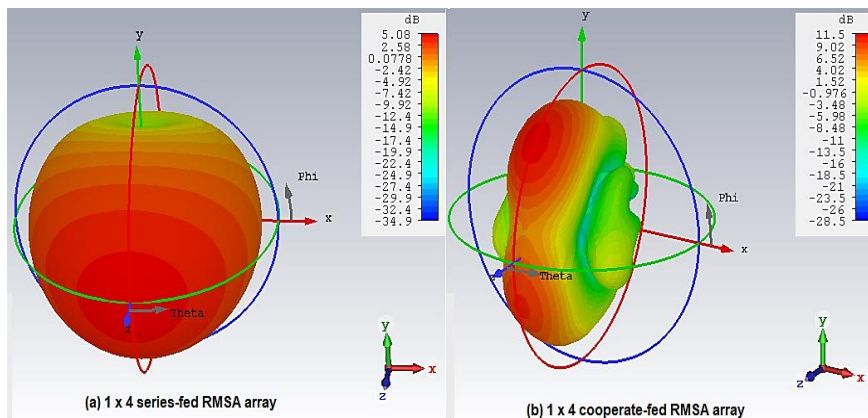


Fig. 29. 3-D gain of proposed 1 x 4 series-fed and 1 x 4 cooperate-fed RMSA array at 2.4 GHz

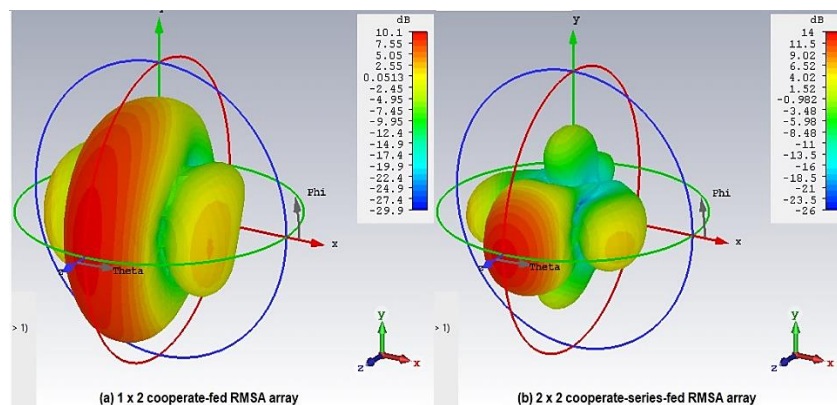


Fig. 30. 3-D gain of proposed 1 x 2 cooperate-fed and 2 x 2 cooperate-series-fed RMSA array at 2.4 GHz

The studied array antennas' results are compared with that of the two single-band antennas, as presented in Table 4. From Table 4, it is observed that the proposed 2 x 2 cooperate-series-fed RMSA array performance in terms of return loss, gain, and bandwidth met the design objectives as it outperforms all other designed antennas in terms of gain and directivity (H-field and E-field), it however fell short in bandwidth performance against the 1 x 4 series-fed RMSA array which had a far superior bandwidth.

Comparison of the 1 x 4 series-fed MSA array by [32] and the proposed 1 x 4 series-fed RMSA was done. Both antennas were designed using FR-4 substrate with dielectric constant (ϵ_r) of 4.2, same feeding method to the primary patch (QWT) and followed up with series-feed thereafter for the subsequent antennas, same substrate height of $h = 1.6$ mm, same characteristic impedance of $Z_o = 50 \Omega$, and at the same frequency of 2.4 GHz. This was done to give room for a balanced antenna parametric performance comparison. The authors' claim of 16 % and 18 % appears inaccurate judging from Equation 33. From computation, the antenna

yielded 4.6% bandwidth against the 6.34 % achieved by the proposed 1 x 4 series-fed RMSA. Their array antenna, however, showed a superior gain performance in comparison to the one proposed in this study.

The array antenna proposed by [18] is compared with the proposed 1 x 4 cooperate-fed MSA array, and the result is as summarised in Table 5.

The proposed 2 x 2 array antenna was also compared with some previously reviewed published journals in Chapter Two of this study, along with other designed antenna arrays, and the summary of the comparison is presented in Table 6. From Table 6, it is evident that all the reviewed works performed well, but none matched the performance of the proposed 2 x 2 RMSA array in terms of gain. Sizes of the different antennas would have been used as a yardstick for comparison only if they were all operating at the same frequency. Also, unlike bandwidth, combined gain performance is not an important measure used for antenna parametric comparison, hence the exclusion of dual-band antenna arrays in the comparison.

Table 4. Comparison of single band antennas and proposed RMSA array antennas

Configuration	Min. S_{11} (dB)	Bandwidth (MHz)	Gain (dB)	Directivity, $\phi = 90^\circ$ (dBi)	Directivity, $\phi = 0^\circ$ (dBi)
Single band - QWT-fed	-19.80	65.30	3.47	6.24	6.16
Single band – Inset-fed	-26.39	68.30	4.85	6.09	6.08
1 x 4 series-fed array	-12.93	152.07	5.08	10.50	5.68
1 x 4 cooperate-fed array	-31.90	44.33	11.50	11.60	7.39
1 x 2 cooperate-fed array	-22.90	33.06	10.10	10.10	10.00
2 x 2 cooperate- and series-fed array	-34.62	50.41	14.00	14.10	14.10

Table 5. Comparison of proposed 1 x 4 cooperate-fed antenna array with Obot et al (2019)

Works	Gain (dBi)	f_r (GHz)	S_{11} (dB)
[18]	10.29	2.4	-8.25
[33]	8.60	2.45	-27.93
proposed 1 x 4 cooperate-fed	11.5	2.4	-31.90

Table 6. Comparison of proposed 2 x 2 antenna array with some selected published works

Antenna	Gain (dBi)	f_r (GHz)	Bandwidth (MHz)
[16]	13.3	2.4	50
[17]	13.2	2.4	30
[18]	10.29	2.4	-
[28]	7.09	2.4	112
[34]	-	10	-
Designed 1 x 4 series-fed	5.08	2.4	152.07
Designed 1 x 4 cooperate-fed	11.5	2.4	44.33
Proposed 2x2 RMSA	14	2.4	50.41

5. CONCLUSION

In this paper, six antennas - two single band RMSAs (QWT-fed and inset-fed), one series-fed 1 x 4 RMA array, two cooperate-fed RMA arrays (1 x 2 and 1 x 4) and a 2 x 2 cooperate-series-fed RMA array at 2.4 GHz – have been designed, simulated and analyzed. Results obtained show that bandwidths of 65.3 MHz and 68.3 MHz which represents 2.72 % and 2.85 % at 2.4 GHz, was achieved by the single band antennas (QWT-fed and Inset-fed). The 1 x 4 arrays (series-fed and cooperate-fed) achieved bandwidths of 152.07 MHz and 44.33 MHz representing 6.34 % and 1.85 %, respectively; while bandwidths of 33.06 MHz and 50.41 MHz which represents 1.38 % and 2.26%.

COMPETING INTERESTS

Authors have declared that no competing interests exist.

REFERENCES

1. Stutzman Warren L, Thiele GA. Antenna Theory and Design, 3rd ed. 2013;53(9). Hoboken, NJ: John Wiley & Sons. DOI:10.1017/CBO9781107415324.004.
2. Technologies W, Engineering E. A triple-band antenna array for next-generation wireless and satellite-based applications. 2014;1–10. DOI:10.1017/S1759078714001275.
3. Singh I, Tripathi VS. Micro strip patch antenna and its applications: A Survey. Int. J. Comput. Technol. Appl. 2011;2(5):1595–1599.
4. Ahmad S, et al. Design of a Tri-Band Wearable Antenna for Millimeter-Wave 5G Applications. Sensors. 2022;22(20). DOI:10.3390/s22208012.
5. Ojaroudi N, Ghadimi N. UWB small slot antenna with WLAN frequency band-stop function. Electron. Lett. 2013;49(21):1317–1318. DOI:10.1049/el.2013.2577.
6. Ojaroudi N. Application of protruded strip resonators to design an UWB slot antenna with WLAN band-notched characteristic. Prog. Electromagn. Res. C. February 2014;47:111–117. DOI:10.2528/PIERC14010606.
7. Ojaroudi Y, Ojaroudi N, Ghadimi N. Irregularly polarized microstrip slot antenna with a pair of spur-shaped slits for wlan applications. Microw. Opt. Technol. Lett. 2015;57(3):756–759. DOI:10.1002/mop.
8. Garg R, Bhartia P, Bahl I, Ittipiboon A. Microstrip antenna design handbook. Norwood, MA: Artech House; 2001.
9. Prabhakaran M, Veeramani R. Comparative analysis of microstrip phased array antenna design. Int. J. Adv. Inf. Sci. Technol. ISSN, 2015;4(11):73–77. DOI:10.15693/ijaist/2015.v4i2.306-310.
10. Balanis CA. Antenna Theory, Analysis and Design., 3rd ed. New Jersey: John Wiley & Sons; 2016.
11. Naveen K, Dasari K, Swapnasri G, Swetha R, Nishitha S, Anusha B. Microstrip patch antenna array with gain enhancement for WLAN applications. Int. Conf. Adv. Smart, Secur. Intell. Comput. Nov. 2022;1–5. DOI:10.1109/ASSIC55218.2022.10088312.
12. Kaur A, Kaur A. Comparative analysis of microstrip patch antennas of different feeding techniques. Int. J. Eng. Dev. Res. 2016;4(4):410–414.
13. Khraisat YSH. Design of 4 elements rectangular microstrip patch antenna with high gain for 2.4 GHz applications. Mod. Appl. Sci. 2011;6(1):68–74. DOI:10.5539/mas.v6n1p68.
14. Alsager AF. Design and analysis of microstrip patch antenna arrays. Msc. Thesis, Univ. Coll. Boras, Sch. Eng. 2011;1:1–80.
15. Ali M, Khawaja BA. Dual band microstrip patch antenna array for next generation wireless sensor network applications,” in proceedings of 2013 International Conference on Sensor Network Security Technology and Privacy Communication System, 2013, no. November 2016;39–43. DOI:10.1109/SNS-PCS.2013.6553831.
16. M. Sohail. Near field focusing of rectangular microstrip patch antenna array; February 2016.
17. Khraisat YSH. Design of 4 elements rectangular microstrip patch antenna with high gain for 2.4 GHz applications,” Mod. Appl. Sci. 2012;6(1):68–74. DOI:10.5539/mas.v6n1p68.
18. Obot AB, Igwue GA, Udofia KM. Design and simulation of rectangular microstrip antenna arrays for improved gain performance. Int. J. Networks Commun. 2019;9(2):73–81. DOI:10.5923/j.ijnc.20190902.02.

19. Sidhu SK, Sivia JS. Analysis and design rectangular patch with half rectangular fractal techniques. *Procedia Comput. Sci.* 2016;85:386–392. DOI:10.1016/j.procs.2016.05.247.
20. Kumar G, Ray KP. *Broadband microstrip antennas.* Artech House; 2003.
21. Huang Y, Boyle K. *Antennas from theory to practice,* 1st ed. West Sussex, United Kingdom: John Wiley & Sons; 2008.
22. Rajendran H. Design of an inset feed rectangular microstrip patch antenna; 2021. DOI:10.1109/APACE53143.2021.9760620.
23. Chemkha H, Belkacem A. Design of new inset fed rectangular microstrip patch antenna with improved fundamental parameters. *DTS 2020 - IEEE Int. Conf. Des. Test Integr. Micro Nano-Systems.* 2020;4:9–12. DOI:10.1109/DTS48731.2020.9196068.
24. Smith LP. Analysis of antenna designs for the maximum power transmission. Georgia Southern University; 2020.
25. Abdullah N, Bhardwaj G, Sunita. Design of squared shape SRR metamaterial by using rectangular microstrip patch antenna at 2.85 GHz,” 2017 4th Int. Conf. Signal Process. Integr. Networks, SPIN. 2017; 196–200. DOI:10.1109/SPIN.2017.8049943.
26. Pozar DM. *Microwave engineering,* 4th Edition,” John Wiley & Sons, Inc. 2012;1–756.
27. Ajay VG, Parvathy AR, Mathew T. Microstrip antenna with DGS based on CSRR array for WiMAX applications,” *Int. J. Electr. Comput. Eng.* 2019;9(1):157. DOI:10.11591/ijece.v9i1.pp157-162.
28. Singh KK, Gupta SC. Review and analysis of microstrip patch array antenna with different configurations. *Int. J. Sci. Eng. Res.* 2013;4(2):1–6.
29. Ramil N, Salleh MK, Md-Tan MN. Reconfigurable rectangular microstrip slot patch antenna using feed line. *IEEE Int. Conf. Syst. Eng. Technol.* 2011;4–5.
30. James JR, Hall PS. *Handbook of microstrip antennas.* Peter Peregrinus, Ltd. 1989;1.
31. Siakavara K. *Methods to design microstrip antennas for modern applications.* Intechopen. 2010;174:184-187.
32. Kumar A, Gupta R. Genetic algorithm in broadband microstrip antenna design. *Int. J. Adv. Res. Comput. Commun.* 2013;2(3): 1469–1472,
33. Reddy D, Reddy R, Mohith, Shilpa B. Design of 4x1 circular microstrip patch array antenna for WLAN applications. *E3S Web Conf.* Jun, 2023;391:01068. DOI:10.1051/E3SCONF/202339101068.
34. Huque T, K. Hosain S, Islam A. Chowdhury, “Design and performance analysis of microstrip array antennas with optimum parameters for X-band applications. *Int. J. Adv. Comput. Sci. Appl.* 2011;2(4):81–87.

© 2024 Ifeanyi et al.; This is an Open Access article distributed under the terms of the Creative Commons Attribution License (<http://creativecommons.org/licenses/by/4.0>), which permits unrestricted use, distribution, and reproduction in any medium, provided the original work is properly cited.

Peer-review history:

The peer review history for this paper can be accessed here:

<https://www.sdiarticle5.com/review-history/111205>